A Generalised Probe Method to Measure the Liquid Complex Permittivity

Lei Xing [1*], Jiajia Zhu [1], Qian Xu [1], Yongjiu Zhao [1], Chaoyun Song [2], Yi Huang [2]

[1] College of Electronic and Information Engineering, Nanjing University of Aeronautics and Astronautics, Nanjing, 21106, China
[2] Department of Electrical Engineering and Electronics, The University of Liverpool, Liverpool, L69 3GJ, UK
[*] xinglei@nuaa.edu.cn

Abstract: A generalised probe method is proposed for fast and accurate complex permittivity measurements. The method is based on the simulated reflection coefficients using the finite difference frequency domain (FDFD) method. A database is setup, which consists of the simulated complex reflection coefficients of the unknown material under test (MUT). A fast searching algorithm is performed to match the measured reflection coefficients to the reference values in the database, thus the complex permittivity of the liquid can be obtained. An in-house measurement system is developed. The unique feature of this system is that it can be applied to an arbitrarily shaped probe. Liquid samples are measured and the results are compared with that published in literatures. Good agreements are obtained. These results could be useful for liquid microwave component designs and applications.

1. Introduction

Recently, liquid materials have been used in microwave devices due to a range of attractive features such as conformability, reconfigurability and transparency. Based on these attractive features, some interesting liquid microwave devices have been reported, including liquid antennas [1-9] (e.g. water based liquid antennas [2, 3], organic liquid antennas [4, 5], ironic liquid antennas [6, 7] and liquid metal antennas [8, 9]), waveguides (e.g. a microfluidically controlled 3D printed waveguide [10]), metamaterials and absorbers (e.g. a water based tunable metasurface [11], a tunable all-dielectric electromagnetic metamaterial [12], and water-based broadband metamaterial absorbers [13,14]).

An accurate measurement of the complex permittivity of the liquid material is necessary, which can provide researchers with valuable information to use the material in most suitable applications (e.g. high conductivity materials can be used for conductive antennas, while high permittivity materials are possible for compact dielectric resonator antennas). Six types of measurement techniques are frequently used in complex permittivity measurement: the open-ended coaxial probe method, the transmission line method, the free space method, the resonant cavity method, the parallel plate method, and the inductance measurement method [15-16]. The choice of measurement technique depends on the material under test (MUT), frequency of interest, the range of permittivity, the required measurement uncertainty, sample size and temperature.

For liquid materials, the open-ended coaxial probe method has been widely used for the attractiveness of broadband measurements, simple sample preparations and easy measurement setup. Efforts have been devoted in this area. In [17, 18], an equivalent circuit of an open-ended coaxial line was used to estimate the permittivity of the MUT, and a fast computation was obtained. In [19-22], analytical full-wave analysis was applied to characterise the permittivity or reflection coefficients of the MUT, providing good accuracy with the expense of simulation time. In [23], an improved model for an open-ended coaxial probe was proposed, which offers a wide range of permittivity measurements without sacrificing computational speed or accuracy. In [24, 25], the open-ended coaxial probe technique was implemented in complex permittivity measurements of artificial sea ice and oil palm fruits, respectively. In [26], a wideband measurement system was developed using coupled coaxial probes, both complex permittivity and permeability can be measured simultaneously. In [27], a developed model for the slim form coaxial probe was presented, which accurately determined the unknown permittivity of human biological tissues. Some commercial products based on the coaxial probe method are also available [28]. Generally, analytical methods are highly complex and may involve infinite series; they also have preconditions and approximations, which may not be suitable for arbitrarily shaped probes (e.g. when the end of a probe is not flat). On the other hand, equivalent circuit model methods simplify the model but the error increases with frequency.

In this paper, a generalised complex permittivity measurement system for liquid materials is developed. This method retains the accuracy of the full-wave method without sacrificing the computation efficiency in measurement. Simulations are carried out by using the finite difference frequency domain (FDFD) method. A database is setup which contains the relationship between the complex reflection coefficients and the material parameters (relative permittivity ε_r and conductivity σ). In the measurement, the reflection coefficient of the MUT is recorded to find the nearest ε_r and σ in the database, and a fast searching algorithm is applied in the matching process. The paper is organised as follows: Section 2 presents the measurement system, theory and algorithm; Section 3 gives the measurement results and

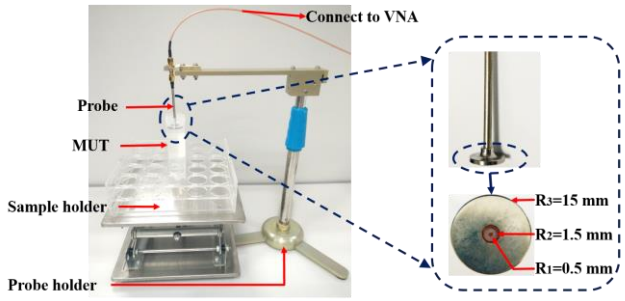

Fig. 1. *Set up of the liquid complex permittivity measurement and geometry of the open-ended coaxial probe.*

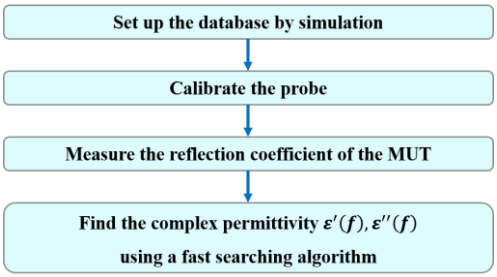

Fig. 2. *Workflow of the proposed measurement system.*

compares them with the published literatures; Section 4 concludes the paper.

2. Measurement system, theory and algorithm

The liquid measurement system consists of a vector network analyser (VNA), an open-ended coaxial probe and control software. The setup of the measurement system and the flanged open-ended coaxial probe with detailed dimensions are presented in Fig. 1. The characteristic impedances of the coaxial probe and the transmission line are 50 Ω. Note that the proposed system is a generalised system and can be applied to an arbitrarily shaped probe, which is the great advantage of the proposed method.

Fig. 2 shows the workflow, the measurement procedure consists of four steps: database setup, calibration, measurement of the MUT and complex permittivity matching using a fast searching algorithm.

2.1. Database Setup

Before measurements, a database is required to record the relationship between the material parameters (relative permittivity ε_r and conductivity σ) and the reflection coefficients. The FDFD method [29, 30] in the commercial software (CST) is applied to simulate the reflection coefficients of the MUT with different values of permittivity. The simulation models are shown in Fig. 3. 21 and 51 samples are collected for ε_r and σ of the MUT, respectively, which can be expressed as:

$$\varepsilon_r = 10^x, \quad x = 0, 0.1, 0.2, \ldots, 2$$
$$\sigma = 10^y, \quad y = -3, -2.9, -2.8, \ldots, 2$$
$$tan\delta = \frac{\varepsilon''}{\varepsilon'} = \frac{\sigma}{\omega \varepsilon_r \varepsilon_0} \tag{1}$$

where ω is angular frequency, ε_0 is vacuum dielectric constant, $tan\delta$ is loss tangent of the material, ε' and ε'' are

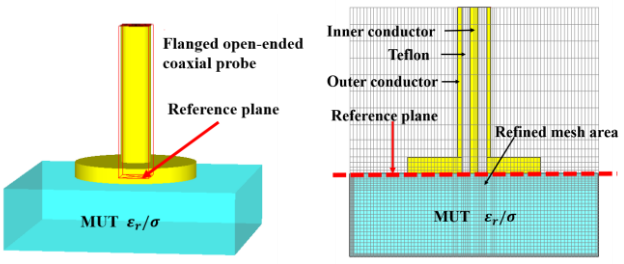

(a) (b)

Fig. 3. *Simulation models of the open-ended coaxial probe and the MUT.* ***(a)*** *Perspective view.* ***(b)*** *Cross-section view (a refined mesh is used at the interface of probe and the MUT).*

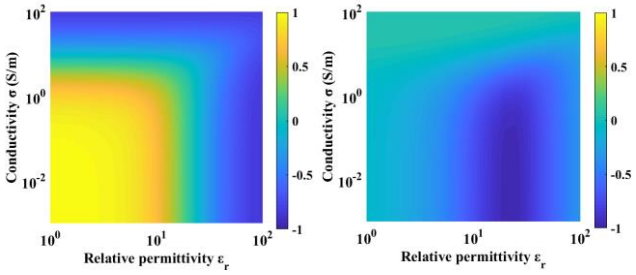

(a) (b)

Fig. 4. *Reflection coefficients with different values of relative permittivity (ε_r) and conductivity (σ) at 6 GHz.* ***(a)*** *Real part.* ***(b)*** *Imaginary part.*

the real part and imaginary part of the complex permittivity, respectively.

The reference plane of the reflection coefficient is set to the end of the probe. 1071 (21×51) samples are simulated, all the reflection coefficients ($\Gamma_{11}(f)$) in the frequency range of 0 - 6 GHz are recorded to form the database. The simulated real part and imaginary part of the reflection coefficients at 6 GHz with different values of ε_r and σ are presented in Fig. 4.

Note that the proposed system is general, the probe dimensions (or the shape of the probe) can be different. If another probe is used, we only need to update the database.

2.2. Calibration

Once the database is setup, the probe calibration should be performed. We need to find the relationship between the measured reflection coefficient (S_{11m}) from the VNA and the reflection coefficient (Γ_r) at the interface between the probe and the MUT (reference plane of the simulated reflection coefficient). The error box (S matrix) between S_{11m} and Γ_r in Fig. 5 can be estimated by the following equations [31]:

$$S_{11s} = e_{11} + \frac{e_{21}e_{12}\Gamma_{rs}}{1 - e_{22}\Gamma_{rs}}$$
$$S_{11o} = e_{11} + \frac{e_{21}e_{12}\Gamma_{ro}}{1 - e_{22}\Gamma_{ro}}$$
$$S_{11w} = e_{11} + \frac{e_{21}e_{12}\Gamma_{rw}}{1 - e_{22}\Gamma_{rw}}$$
$$e_{21} = e_{12} \tag{2}$$

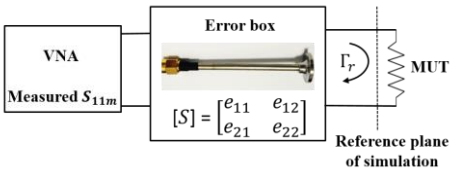

Fig. 5. *Block diagram of the error box.*

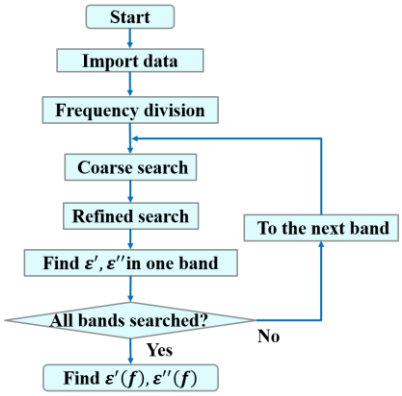

Fig. 6. *Flow chart of the fast searching algorithm.*

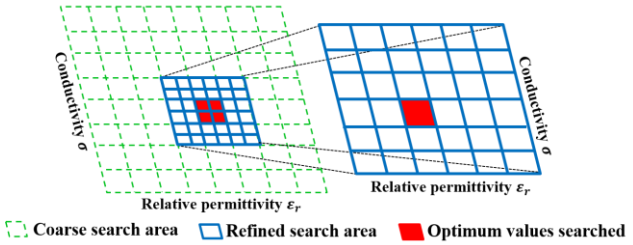

Fig. 7. *Coarse search and refined search.*

where S_{11s} , S_{11o} and S_{11w} are the measured reflection coefficients of short, open, and pure water, Γ_{rs}, Γ_{ro}, and Γ_{rw} are the simulated reflection coefficients of short, open, and pure water in the database.

A three-step calibration procedure is performed. Three different loadings including open, short and material with known permittivity (pure water) are used. According to (2), the corresponding measured reflection coefficient (S_{11s}, S_{11o} and S_{11w}) recorded from the VNA and the reflection coefficient (Γ_{rs}, Γ_{ro}, and Γ_{rw}) obtained from the simulations are utilized to solve the error box as:

$$e_{11} = [S_{11w}\Gamma_{ro}\Gamma_{rs}(S_{11s} - S_{11o}) - S_{11o}\Gamma_{rw}\Gamma_{rs}(S_{11s} - S_{11w}) + S_{11s}\Gamma_{ro}\Gamma_{rw}(S_{11o} - S_{11w})]/\Delta$$

$$e_{12} = e_{21} = [(S_{11s} - S_{11o})(S_{11s} - S_{11w})(S_{11o} - S_{11w})(\Gamma_{rs} - \Gamma_{ro})(\Gamma_{rs} - \Gamma_{rw})(\Gamma_{ro} - \Gamma_{rw})]^{\frac{1}{2}}/\Delta$$

$$e_{22} = [-\Gamma_{rw}(S_{11s} - S_{11o}) + \Gamma_{ro}(S_{11s} - S_{11w}) - \Gamma_{rs}(S_{11o} - S_{11w})]/\Delta$$

$$\text{where } \Delta = \Gamma_{rs}\Gamma_{ro}(S_{11s} - S_{11o}) - \Gamma_{rs}\Gamma_{rw}(S_{11s} - S_{11w}) + \Gamma_{ro}\Gamma_{rw}(S_{11o} - S_{11w}) \quad (3)$$

2.3. MUT Measurement

Since the error box is known, when the reflection coefficient of MUT is measured, reflection coefficient at MUT interface Γ_r can be obtained in an inverse way:

$$\Gamma_r = \frac{e_{11} - S_{11m}}{e_{11}e_{22} - e_{21}^2 - e_{22}S_{11m}} \quad (4)$$

where S_{11m} is the measured reflection coefficient of the MUT using VNA.

2.4. Fast Searching Algorithm

The complex permittivity is evaluated using a fast searching algorithm after measuring the reflection coefficient of MUT. Considering the frequency dependency of the material property, the matching process is performed in a sequence of frequency bands as shown in Fig. 6. In each frequency band, two kinds of search are applied: a coarse search with 1071 samples and a refined search in a smaller region. We repeat the matching process in the refined region, thus ε' and ε'' (the nearest values) of the MUT can be found. The searching process is illustrated in Fig. 7. The searching algorithm is very similar to the quadtree algorithm in computer science [32]. By comparing the reflection coefficient of MUT (Γ_r) and that in database ($\Gamma_{11}(f)$), a sample with the minimum average error can be searched. The error of a single frequency ($\mathrm{Err}(f)$) and the average error ($\langle \mathrm{Err}(f) \rangle$) are defined as:

$$\mathrm{Err}(f) = |S_{11\mathrm{ReMUT}} - S_{11\mathrm{ReRef}}| + |S_{11\mathrm{ImMUT}} - S_{11\mathrm{ImRef}}|$$
$$\langle \mathrm{Err}(f) \rangle = [\mathrm{Err}(f_1) + \mathrm{Err}(f_2) + \cdots + \mathrm{Err}(f_n)]/n \quad (5)$$

where $S_{11\mathrm{ReMUT}}$ and $S_{11\mathrm{ImMUT}}$ are the real and imaginary part of the measured reflection coefficient of MUT, respectively. $S_{11\mathrm{ReRef}}$ and $S_{11\mathrm{ImRef}}$ are the real and imaginary part of simulated reflection coefficient in database, respectively. f_1, f_2 and f_n are the frequency points in the band, and n is the number of frequency points.

The measurement process is less than 1 second and the searching time is less than 2 seconds (for a relative bandwidth of 10% in matching process), which is much faster than the full-wave analysis.

3. Measurement Results

To validate the system, measurements were carried out for different liquid materials, including salty water, water with PG (propylene glycol), water with ethanol and pure ethyl acetate. Each sample was measured at room temperature (25 ℃), 1001 frequency points from 100 kHz to 6 GHz were measured. The measurement results are compared with those in the published literatures in Table 1. Fig. 8 shows the reflection coefficients before and after calibration of one liquid sample (pure ethyl acetate). As expected, the reference plane of the reflection coefficient is transformed to the interface between the probe and the MUT.

The complex permittivity of the four liquids are shown in Fig. 9 - Fig. 12, which are compared with those in published literatures. Good agreements are achieved. It can be seen that the four liquids have different electrical properties and can be applied in various applications. The salty water (salinity 50 ppt) has an imaginary part higher

Table 1 Comparison of measurement and published results

Liquid samples	Measurement results	Published literatures
Salty water (salinity 50 ppt)	Fig. 9	[33]
Water with 5% PG	Fig. 10	[34]
Water with 60% ethanol	Fig. 11	[35]
Pure ethyl acetate	Fig. 12	[36]

(ppt: parts per thousand)

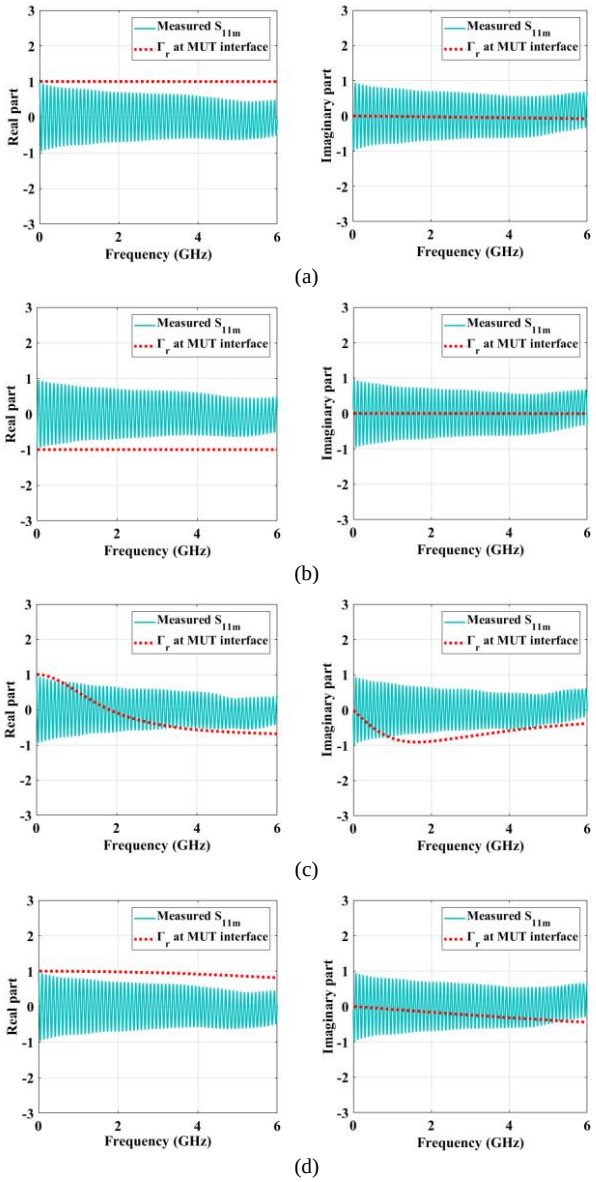

Fig. 8. *Calibration process by using:* ***(a)*** *open,* ***(b)*** *short and* ***(c)*** *pure water.* ***(d)*** *Measured reflection coefficients of MUT (pure ethyl acetate).*

than 38, which could be used as a conductive material. The water with 5% PG has a similar permittivity with the pure water; In the meanwhile, it has a freezing point around −3 ℃, which can replace the pure water at low temperatures. The pure ethyl acetate has a real part around 6 and an imaginary part less than 0.8, which is a promising candidate for dielectric loaded applications.

In Fig. 9 - Fig. 12, we can observe small differences

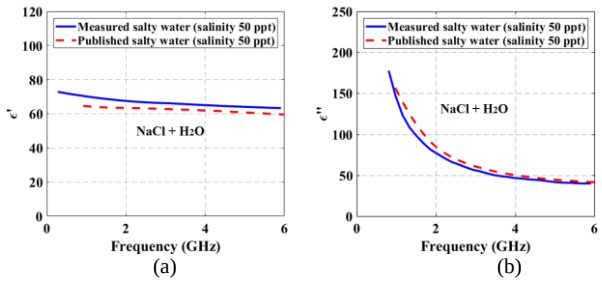

Fig. 9. ***(a)*** *Real part and* ***(b)*** *imaginary part of the complex permittivity of the salty water (salinity 50 ppt) at* 25℃.

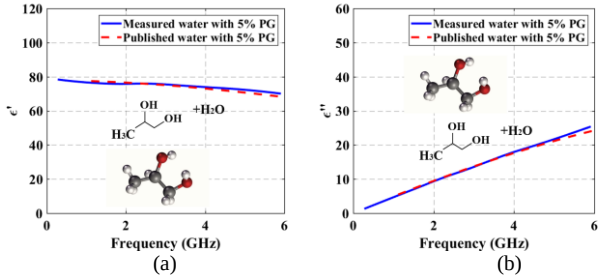

Fig. 10. ***(a)*** *Real part and* ***(b)*** *imaginary part of the complex permittivity of the water with 5% PG at* 25 ℃.

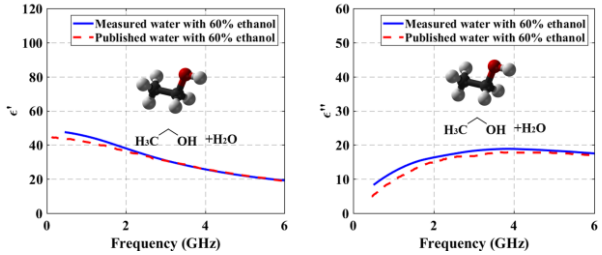

Fig. 11. ***(a)*** *Real part and* ***(b)*** *imaginary part of the complex permittivity of the water with 60% ethanol at* 25 ℃.

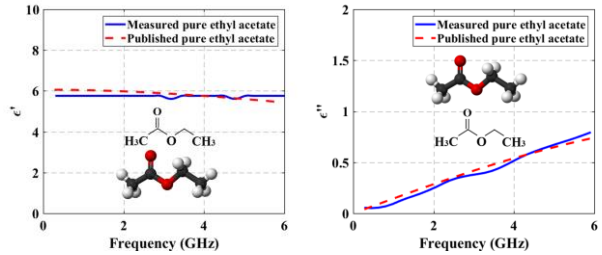

Fig. 12. ***(a)*** *Real part and* ***(b)*** *imaginary part of the complex permittivity of the pure ethyl acetate at* 25 ℃.

between the measured and published results. This should be due to the manufacture error of the probe. It could also be due to the different models and the instrument uncertainties used in the material measurement. Note that the simulated model in this paper is full wave and very accurate, the error could be dominated by the manufacture error.

4. Conclusion

In this paper, a generalised system has been proposed for complex permittivity measurement of liquid materials. The system has advantages of high efficiency, broadband measurement and can be applied to an arbitrarily shaped

probe. It provides a new approach for complex permittivity measurement of liquid materials. By comparing measurement results with published literatures, the system has been verified. Typical liquid samples have been measured, and potential applications of these samples have been discussed.

5. Acknowledgments

This work was supported in part by the National Natural Science Foundation of China under Grant 61601219 and Nature Science Foundation of Jiangsu Province under Grant BK20160804.

6. References

[1] Zou, M., Hu, Z., Hua, C., et al.: 'Liquid antennas', in Wiley Encyclopedia Electrical and Electronics Engineering, 2016, pp. 1-37

[2] Mobashsher, A. T., Abbosh, A.: 'Reconfigurable water-substrate based antennas with temperature control', Appl. Phys. Lett., 2017,110, 253503

[3] Li, Y., Luk, K. M.: 'A water dense dielectric patch antenna', IEEE Access, 2015, 3, pp. 274-28

[4] Chen, Z., Wong, H.: 'Liquid dielectric resonator antenna with circular polarization reconfigurability', IEEE Trans. Antennas Propag., 2018, 66, (1), pp. 444-449

[5] Chen, Z., Wong, H.: 'Wideband glass and liquid cylindrical dielectric resonator antenna for pattern reconfigurable design', IEEE Trans. Antennas Propag., 2017, 65, (5), pp. 2157-2164

[6] Song, C. Y., Bennett, E. L., Xiao, J. L., et al.: 'Compact ultra-wideband monopole antenna using novel liquid loading materials', IEEE Access, 2019, 7, pp. 49039-49047

[7] Song, C. Y., Bennett, E. L., Xiao, J. L., et al.: 'Metasurfaced, broadband and circularly polarized liquid antennas using a simple structure', IEEE Trans. Antennas Propag., 2019, 67, (7), pp. 4907-4913

[8] Wang, M., Khan, M. R., Dickey, et al.: 'A compound frequency and polarization reconfigurable crossed dipole using multidirectional spreading of liquid metal', IEEE Antennas Wireless Propag. Lett., 2017, 16, pp. 79-82

[9] Zhang, G. B., Gough, R. C., Moorefield, M. R., et al.: 'A liquid metal polarization-pattern-reconfigurable dipole antenna', IEEE Antennas Wireless Propag. Lett., 2018, 17, (1), pp. 50-53

[10] Khan, S., Vahabisani, N., Daneshmand, M.: 'A fully 3-D printed waveguide and its application as microfluidically controlled waveguide switch', IEEE Trans. Compon., Packag., Manuf. Technol., 2017, 7, (1), pp. 70-80

[11] Odit, M., Kapitanova, P., Andryieuski, A., et al.: 'Experimental demonstration of water based tunable metasurface', Appl. Phys. Lett., 2016,109, 011901

[12] Andryieuski, A., Kuznetsova, S. M., Zhukovsky, S.V., et al.: 'Water: promising opportunities for tunable all-dielectric electromagnetic metamaterials', Sci. Rep., 2015, 5, 13535

[13] Zhao, J., Wei, S., Wang, C., et al.: 'Broadband microwave absorption utilizing water-based metamaterial structures', Opt. Express, 2018, 26, (7), 8522-8531

[14] Pang, Y., Shen, Y., Li, Y., et al.: 'Water-based metamaterial absorbers for optical transparency and broadband microwave absorption', J. Appl. Phys., 2018, 123, 155106

[15] Venkatesh, M. S., Raghavan, G. S. V.: 'An overview of dielectric properties measuring techniques', Can. Biosyst. Eng., 2005, 47, pp. 7.15-7.30

[16] Basics of measuring the dielectric properties of materials, Keysight literature number: 5989-2589 EN, 2015

[17] Athey, T. W., Stuchly, M. A., Stuchly, S. S.: 'Measurement of radio frequency permittivity of biological tissues with an open-ended coaxial line: Part I', IEEE Trans. Microw. Theory Tech., 1982, 30, (1), pp. 82-86

[18] Gajda, G., Stuchly, S. S.: 'An equivalent circuit of an open-ended coaxial line', IEEE Trans. Instrum. Meas., 1981, 32, (4), pp. 506-509

[19] Li, C. L., Chen, K. M.: 'Determination of electromagnetic properties of materials using flanged open-ended coaxial probe full-wave analysis', IEEE Trans. Instrum. Meas, 1995, 44, (1), pp. 19-27

[20] Panariello, G., Verolino, L., Vitolo, G.: 'Efficient and accurate full wave analysis of the open ended coaxial cable', IEEE Trans. Microw. Theory Tech., 2001, 49, (7), pp. 1304-1309

[21] Hayashi, Y., Oba, K., Hirayama, K.: 'Application of FEM to measurement of permittivity and permeability of lossy sheet using coaxial line', Electron. Commun. Jpn., 2005, 88, (9), pp. 10-18

[22] Huang, R., Zhang, D.: 'Analysis of open-ended coaxial probes by using a two-dimensional finite-difference frequency-domain method', IEEE Trans. Instrum. Meas., 2008, 57, (5), pp. 931-939

[23] Blackham, D. V., Pollard, R. D.: 'An improved technique for permittivity measurements using a coaxial probe', IEEE Trans. Instrum. Meas., 1997, 46, (5), pp. 1093-1099

[24] Komarov, S. A., Komarov, A. S., Barber, D. G., et al.: 'Open-ended coaxial probe technique for dielectric spectroscopy of artificially grown sea ice', IEEE Trans. Geosci. Remote Sens., 2016, 54, (8), pp. 4941-4951

[25] Abbas, Z., Yeow, Y. K., Shaari, A. H., et al.: 'Complex permittivity and moisture measurements of oil palm fruits using an open ended coaxial sensor', IEEE Sensors J., 2005, 5, (6), pp. 1281-1287

[26] Hosseini, M. H., Heidar, H., Shams, M. H.: 'Wideband nondestructive measurement of complex permittivity and permeability using coupled coaxial probes', IEEE Trans. Instrum. Meas., 2017, 66, (1), pp. 148-157

[27] Sabzevari, A. M., Tavassolian, N.: 'Characterization and validation of the slim form open ended coaxial probe for the dielectric characterization of biological tissues at millimeter wave frequencies', IEEE Microw. Wireless Compon. Lett., 2018, 28, (1), pp. 85-87

[28] Keysight Technologies: N1500A Web Help, http://:www.Keysight.com/find/Materials, accessed 3 December 2014

[29] Christ A., Hartnagel H. L.: 'Three dimensional finite difference method for the analysis of microwave device embedding', IEEE Trans. Microw. Theory Tech., 1987, 35, (8), pp. 88-696

[30] Ling R. T.: 'A finite-difference frequency domain (FD-FD) approach to electromagnetic scattering problem', J. Electromagnet. Wave, 1989, 3, (2), pp. 107-128
[31] Pozar, D. M.: 'Microwave Engineering' (Wiley, 2012), pp. 97
[32] Samet, H.: 'The quadtree and related hierarchical data structures', ACM Computing Surveys, 1984, 16, (2), pp. 187-260
[33] Xing, L.: 'Investigations of water-based liquid antennas for wireless communications', PhD thesis, University of Liverpool, 2015
[34] Xing, L., Huang, Y., Xu, Q., et al.: 'Complex permittivity of water-based liquids for liquid antennas', IEEE Antennas Wireless Propag. Lett., 2016, 15, pp. 1626-1629
[35] Bao, J. Z., Swicord, M. L., Davis, C. C.: 'Microwave dielectric characterization of binary mixtures of water, methanol, and ethanol', J. Chem. Phys., 1996, 104, (12), pp. 4441-4450
[36] Shirke, R. M., Chaudhari, A., More, N. M., et al.: 'Temperature dependent dielectric relaxation study of ethyl acetate-alcohol mixtures using time domain technique', J. Mol. Liq., 2001, 94, (1), pp. 27-36.